A congenital activating mutant of WASp causes altered plasma membrane topography and adhesion under flow in lymphocytes

Siobhan O. Burns,[1,2] David J. Killock,[3] Dale A. Moulding,[1] Joao Metelo,[1] Joao Nunes,[1] Ruth R. Taylor,[4] Andrew Forge,[4] Adrian J. Thrasher,[1,2] and Aleksandar Ivetic[3]

[1]Molecular Immunology Unit, Centre for Immunodeficiency, Institute of Child Health, University College London (UCL), London; [2]Great Ormond Street Hospital for Children, National Health Service (NHS) Trust, London; [3]Cytoskeleton/Membrane Signalling Group, Cardiovascular Division, British Heart Foundation (BHF) Centre for Research Excellence, James Black Centre, King's College London, London; and [4]Centre for Auditory Research, UCL Ear Institute, London, United Kingdom

Leukocytes rely on dynamic actin-dependent changes in cell shape to pass through blood vessels, which is fundamental to immune surveillance. Wiskott-Aldrich Syndrome protein (WASp) is a hematopoietic cell–restricted cytoskeletal regulator important for modulating cell shape through Arp2/3-mediated actin polymerization. A recently identified WASp^{I294T} mutation was shown to render WASp constitutively active in vivo, causing increased filamentous (F)–actin polymerization, high podosome turnover in macrophages, and myelodysplasia. The aim of this study was to determine the effect of WASp^{I294T} expression in lymphocytes. Here, we report that lymphocytes isolated from a patient with WASp^{I294T}, and in a cellular model of WASp^{I294T}, displayed abnormal microvillar architecture, associated with an increase in total cellular F-actin. Microvillus function was additionally altered as lymphocytes bearing the WASp^{I294T} mutation failed to roll normally on L-selectin ligand under flow. This was not because of defects in L-selectin expression, shedding, cytoskeletal anchorage, or membranal positioning; however, under static conditions of adhesion, WASp^{I294T}-expressing lymphocytes exhibited altered dynamic interaction with L-selectin ligand, with a significantly reduced rate of adhesion turnover. Together, our results demonstrate that WASp^{I294T} significantly affects lymphocyte membrane topography and L-selectin–dependent adhesion, which may be linked to defective hematopoiesis and leukocyte function in affected patients. (*Blood*. 2010;115(26):5355-5365)

Introduction

The Wiskott-Aldrich Syndrome protein (WASp) is a key cytoskeletal regulator in hematopoietic cells.[1] Through its multidomain structure, WASp integrates inputs from disparate signaling pathways to initiate and regulate Arp2/3-mediated actin polymerization. This is important for the normal formation of various actin-rich structures including the T-cell immune synapse, phagocytic cups, and specialized adhesion structures called podosomes in myeloid cells.[2-4] The majority of human disease-causing mutations in WASp are hypomorphic or null loss of function mutations, which result in Wiskott-Aldrich Syndrome (WAS).[5] Patients with WAS classically suffer from thrombocytopenia, eczema, and a broad immunodeficiency, reflecting the functional deficiency of almost all hematopoietic lineages.

Recently, 3 novel human mutations (L270P, S272P, and I294T) leading to constitutive WASp activation have been reported to cause a distinct disease, X-linked neutropoenia (XLN).[6,7] All 3 are positioned in the GTPase binding domain (GBD; residues 230-288) of WASp and disrupt its autoinhibitory interaction with the Arp2/3 binding, C-terminal verprolin homology, central, acidic (VCA) domain. The result is enhanced and dysregulated WASp activity characterized by an increase in cellular filamentous (F)–actin and abnormalities of actin cytoskeletal structure and dynamics. A large kindred bearing the rare I294T mutation was recently reported, informing our understanding of the clinical spectrum of WASp^{I294T} disease, which appears variable but is usually associated with neutropoenia and recurrent infections.[7,8] Although fatal infections have been described, infectious complications are surprisingly mild and not correlated with the degree of neutropoenia.[8] Other immunopathology is also seen, including low levels of CD4 and CD8 T cells, natural killer (NK) cell and B-cell lymphopenia, and reduced levels of IgA. To date, specific cellular effects have only been examined in myeloid cells, where defects of myelopoiesis and podosome formation have been reported.[7,9] Our aim in this report was to determine whether WASp^{I294T} also attenuates aspects of lymphocyte function.

The lymphocyte surface is dominated by microvilli: prominent actin-rich, fingerlike membrane projections involved in mediating cell-cell interactions.[10] Despite some controversy in the literature, WASp appears to be required for normal microvillar formation in human lymphocytes.[11-16] Microvilli are abundant on most circulating leukocytes and are enriched in signaling proteins, such as k-Ras and Rap1A,[17] which are ultimately involved in facilitating the migration of leukocytes from the blood in to surrounding tissue during inflammation.[18] One of the main purposes of microvilli in circulating leukocytes is to partition cell adhesion molecules into distinct microdomains of the plasma membrane. For example, cell adhesion molecules involved in leukocyte tethering and rolling such as L-selectin are anchored to microvilli, whereas cell adhesion

Submitted August 3, 2009; accepted March 8, 2010. Prepublished online as *Blood* First Edition paper, March 30, 2010; DOI 10.1182/blood-2009-08-236174.

An Inside *Blood* analysis of this article appears at the front of this issue.

The online version of this article contains a data supplement.

The publication costs of this article were defrayed in part by page charge payment. Therefore, and solely to indicate this fact, this article is hereby marked "advertisement" in accordance with 18 USC section 1734.

molecules such as β_2 integrins reside on the cell body[19] and are involved in migration on top of, through, and between individual endothelial cells. These characteristic stages of transmigration occur once the leukocyte has become activated by chemoattractants, which leads to collapse of microvilli and subsequent cell polarization.[20] Thus, dynamic regulation of microvillus assembly is critical for lymphocyte homing.

Here, we report that expression of WASp^{I294T} in primary lymphocytes derived from a patient with XLN or in a lymphocyte cell line promotes the abnormal formation of microvilli as observed using scanning electron microscopy (SEM). This altered phenotype did not affect the surface distribution, expression levels, or cytoskeletal attachment of L-selectin, but did affect adhesion to an L-selectin–specific ligand under flow. Interference reflection microscopy (IRM) studies revealed that adhesion of L-selectin to its ligand induced rapid membrane turnover in cells expressing wild-type (WT) WASp, which was significantly reduced in cells expressing WASp^{I294T}. These findings provide insights into the mechanisms by which WASp^{I294T} promotes defective L-selectin–dependent rolling and suggest that altered adhesion dynamics could be linked to defective hematopoesis or immunopathology associated with XLN.

Methods

Cell lines and patient samples

The previously described[21] 300.19 murine pre-B lymphoma cell line stably expressing human L-selectin was cultured at 37°C/5% CO_2 in RPMI-1640 (Invitrogen) containing 10% fetal calf serum, 50μM β-mercaptoethanol, and 2.5 μg/mL puromycin (Sigma), and was maintained at a density of 0.5 to 1.0 × 10^6 cells/mL.

Peripheral blood was obtained from 1 patient with WASp^{I294T} and 4 healthy donors with informed written consent in accordance with the Declaration of Helsinki and ethical approval from the Great Ormond Street Hospital for Children and the Institute of Child Health Research Ethics. Peripheral blood mononuclear cells (PBMCs) were collected using Histopaque-1077 separation and washed in RPMI-1640. T-lymphocytes were isolated using magnetic bead negative selection kits (Miltenyi Biotec) according to the manufacturer's instructions. Purity and L-selectin levels were measured by flow cytometry (DakoCyAN; Beckman Coulter) after labeling with antibodies against human CD3 (BD Biosciences) and L-selectin (DREG56; Santa Cruz Biotechnology) on ice for 30 minutes. Data were analyzed using FlowJo software (TreeStar).

Lentivirus generation and transduction of 300.19 cells

Lentiviral vectors expressing enhanced green fluorescent protein (EGFP; sometimes called SEW in "Results" to denote vector components, namely spleen-focus forming virus promoter, EGFP, and woodchuck hepatitis posttranscriptional regulatory element), EGFP fused to human WASp, and EGFP fused to the N-terminus of human WASp with the I294T mutation were cloned in to the pHR′SIN-cPPT-SE lentiviral backbone vector as described previously.[22] Virus was titred by measuring the percentage of transduced HT1080 cells expressing EGFP fluorescence. A total of 2 × 10^5 300.19 cells were cultured with lentivirus at a multiplicity of infection (MOI) of 10 to generate stably transfected cell lines. EGFP$^+$ cells were selected by flow-assisted cell sorting (FACS) to give a homogenous population of EGFP-expressing cells. EGFP levels were analyzed using a Cyan flow cytometer (Beckman Coulter) and Summit software (DakoCytomation).

Measurement of actin polymerization

Untransduced and transduced 300.19 cells were mixed (1:1 ratio), fixed in 4% paraformaldehyde (Polysciences Inc) in phosphate-buffered saline (PBS), permeabilized with Perm/Wash (BD Biosciences), and incubated with 5 U/mL rhodamine-phalloidin (Molecular Probes) for 30 minutes on ice. After washing in Perm/Wash buffer, cells were analyzed with a Cyan flow cytometer and Summit software. The difference in phalloidin staining between EGFP$^+$ and EGFP$^-$ cells in the same sample was calculated using Summit Version 4.1 software.

Western blotting

Antibodies used were as follows: anti-WASp (clone B9; Santa Cruz Biotechnology), anti-actin (Sigma-Aldrich), horseradish peroxidase–conjugated secondary antibody (GE Healthcare), anti-ERM, and anti–phospho-ERM (Cell Signaling). For full methodology, see supplemental Methods (available on the *Blood* Web site; see the Supplemental Materials link at the top of the online article).

SEM

After overnight incubation in serum-free RPMI-1640, 300.19 cells or human PBMCs were fixed and prepared for scanning electron microscopy (SEM) as described in supplemental Methods. Images were captured using a JEOL 6100 SEM operating at 15 kV with Semafore software and processed with Adobe Photoshop. For quantification, images were assigned a random number, and cell morphology was scored blindly by 2 independent researchers. Microvilli were judged to be dense, rather than normal, if cell membrane was not visible between microvilli. Results were analyzed using a 2-tailed Fisher test.

Immunogold staining

After being serum-starved for 4 hours, 300.19 cells were labeled with anti–L-selectin antibody (DREG 56) on ice for 30 minutes, then conjugated with secondary antibody to 10-nm immunogold particles (BB International) for 45 minutes on ice. Cells were washed and plated onto poly-L-lysine (PLL; Sigma)–coated coverslips, incubated at room temperature for 20 minutes, and fixed and prepared as described in supplemental Methods. Images were captured using a JEOL 6700F field emission–scanning electron microscope (FESEM) and JEOL software and analyzed with Adobe Photoshop. To calculate the proportion of the cell surface represented by surface protrusions, the image was assessed at maximum contrast. Projections appeared as white pixels, whereas the cell body appeared black. For each micrograph, the number of pixels with an intensity level of 225 to 127.5 (light gray–white) and 127.5 to 0 (black–dark gray) were calculated and expressed as a ratio.

PMA-induced shedding assays

A total of 1 × 10^6 300.19 cells were treated in growth medium supplemented with either phorbol myristate acetate (PMA; Sigma-Aldrich) or equivalent amounts of the appropriate carrier (ie, DMSO) at 37°C/5% CO_2 for 30 minutes. Primary T-lymphocytes were incubated with anti-CD3/CD28 beads (Miltenyi Biotec) or 30μM sheddase inhibitor (Ro-31-9790; kind gift from Dr Ann Ager, Cardiff, United Kingdom) in RPMI-1640 at 37°C/5% CO_2 for 60 minutes. Cells were washed and labeled with either FITC- or PE-labeled DREG56 or IgG_1 isotype control (1:80 in 50 μL for 300.19 cells and 1:20 in 100 μL for primary cells) for 30 minutes on ice. Flow cytometry was performed (DakoCyAN; Beckman Coulter). For 300.19 experiments, data were represented as percentage of L-selectin remaining relative to carrier-only treated cells after correction for background fluorescence (isotype control).

Parallel plate flow chamber assay

Nunc Slide Flaskettes (9 cm^2; Nalge Nunc International) were disassembled to use the slide for rolling assays. Sialyl Lewis-X (sLe^x; GlycoTech) was prepared as previously described[23] (see supplemental Methods for more information). Excess sLe^x was removed by aspiration and gentle washing with PBS, after which slides were blocked in PBS/1% bovine serum albumin (BSA) for 2 hours at room temperature. Slides were washed twice with PBS, mounted in a chamber slide-base parallel plate

flow chamber (channel height 0.15 cm; custom made by Imperial College London) and visualized as previously described[21] (full details in supplemental Methods). The 300.19 cells were resuspended at a density of 3×10^5/mL in Hanks balanced salt solution (HBSS) and 2% BSA (viscosity 0.007 poise) and perfused at 37°C over sLe^x-coated slides at a fixed shear stress of 2.5 dyn/cm^2. Rolling cells were defined as those with a mean velocity between 3 and 200 μm/s; adherent cells were specified as those moving less than 3 μm within a 10-second time period. Mean rolling velocity was calculated from measurements of at least 300 cells in each independent experiment (unless otherwise stated). Jerkiness was measured by tracking individual cell displacement events, which occurred in the direction of flow, every 0.07 seconds over 8 to 10 seconds.

IRM measurements

Coverslips were coated with PLL or sLe^x as described. A total of 1×10^5 cells were allowed to adhere for 5 minutes. Coverslips were then inverted onto glass chambers containing normal growth medium, sealed with wax, and maintained at 37°C for imaging. As previously described,[24] IRM images were collected using a Zeiss Standard 18 microscope with IV-FL incident light fluorescence attachment, appropriate filters for IRM acquisition, and a Zeiss 63×/1.25 NA Neofluar Antiflex oil-immersion objective. Images were collected digitally with a computer-controlled shutter every 2 seconds for 30 frames using a Pulnix charge-coupled device (CCD) camera (Jai Ltd) coupled to a Matrox Meteor PCI frame grabber and in-house acquisition software (Matrox Video and Imaging Technology Europe Ltd). Images were saved as stacked TIFF files and separated into individual TIFF files using ImageJ software (National Institutes of Health). Persistence of contact sites was analyzed using Adobe Photoshop, according to a previously described methodology[24] (full details in supplemental Methods).

Results

Aberrant microvillar architecture and L-selectin–dependent adhesion in PBMCs derived from a patient with WASp^{I294T}

We have previously described a patient bearing the WASp^{I294T} mutation, which is predicted to disrupt the normal autoinhibition mechanism (Figure 1A).[7] To investigate the effect of WASp^{I294T} on lymphocyte surface topography, PBMCs were freshly prepared from this patient and 2 healthy donors and examined by SEM. As expected, the majority of cells both from healthy donors and our patient contained abundant microvilli—typical of lymphocytes[16] (Figure 1B). Although heterogeneity was apparent in both healthy donor and patient cell populations, a significantly higher proportion of WASp^{I294T} lymphocytes displayed unusually dense microvilli ($P < .05$; Figure 1B arrowheads; Figure 1C). In these cells, no areas of cell body were visible between microvilli (Figure 1B), indicating that constitutively active WASp is involved in aberrant maintenance of microvillar formation. In addition, microvilli in WASp^{I294T} lymphocytes appeared broad and dysmorphic (Figure 1B arrows).

To determine the functional significance of these findings, L-selectin–dependent adhesion was tested under flow conditions. Using a parallel plate flow chamber, cells were monitored for rolling behavior by perfusion over immobilized sLe^x as described in "Parallel plate flow chamber assay." Although WASp^{I294T} and healthy donor PBMCs expressed similar levels of surface L-selectin (Figure 2A), the average rolling velocity for WASp^{I294T} cells was higher than that measured for healthy controls (Figure 2B). Similar proportions of cells were scored as rolling in free flow or adherent in both patient and control samples (data not shown). These findings were not due to differences in cell subpopulations within the PBMC fractions, as the same findings were observed in purified T cells (supplemental Figure 1). Closer inspection of rolling behavior between patient and control cells revealed that the WASp^{I294T} cells rolled with a more "jerky" nature compared with control cells, as evidenced by large fluctuations in rolling velocity over time (Figure 2C). Indeed, "jerky" rolling cells periodically achieved velocities that were higher than the normal rolling speed between periods of low velocity typical of rolling cells (supplemental Figure 1D). These results suggest that contacts between L-selectin and ligand were abnormally formed under flow and demonstrate a defect of L-selectin–dependent adhesion in primary WASp^{I294T} lymphocytes.

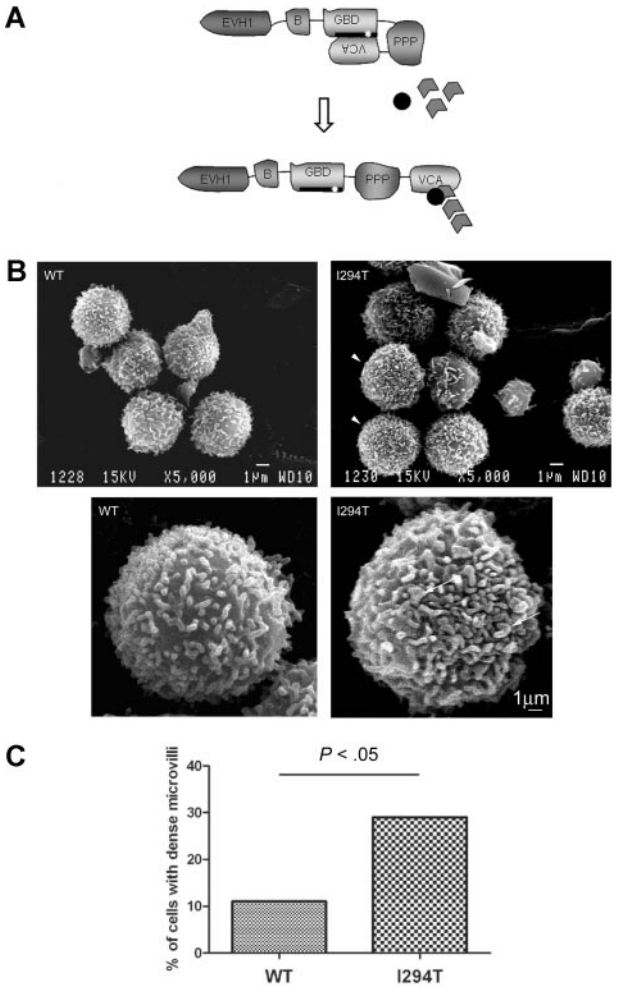

Figure 1. WASp^{I294T} lymphocytes demonstrate dysmorphic microvilli. (A) Schematic showing the modular domain structure of WASp. Before activation, WASp adopts an autoinhibited conformation in which intramolecular interaction of the VCA and GBD domains prevents binding of the Arp2/3 complex and monomeric actin to the carboxy terminus. The I294T mutation (white star) lies in the critical VCA binding region (thick black line; amino acids 242-310) and is predicted to disrupt VCA interaction, resulting in constitutive activation. (B) SEM micrographs of lymphocytes from a healthy donor (WT) and a patient with WASp^{I294T}. WASp^{I294T} cells show dense and frequently dysmorphic microvilli (arrowheads and arrows). Scale bars represent 1 μm. Images were acquired using a JEOL 6100 SEM operating at 15 kV and captured using Semafore software and processed (crop and brightness/contrast functions only) with Adobe Photoshop. (C) Lymphocytes were scored blindly for dense microvilli by 2 independent observers. At least 50 cells were scored for each of WASp^{WT} and WASp^{I294T} cells. A significantly greater percentage of WASp^{I294T} cells assembled dense microvilli ($P < .05$ Fisher exact 1-tailed test).

Generation of stable cell lines expressing WASp and L-selectin

Because primary human WASp^{I294T} cells were not readily accessible, and to examine the mechanism for attenuated L-selectin–

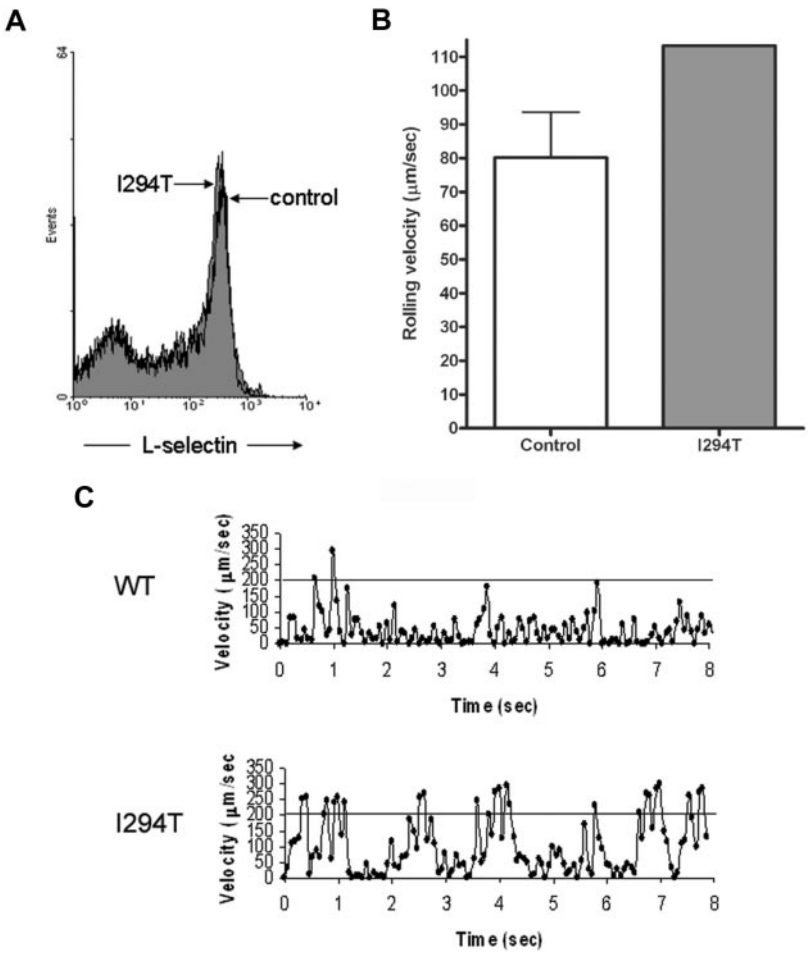

Figure 2. WASp^{I294T} PBMCs demonstrate defective L-selectin–dependent rolling despite normal levels of surface L-selectin. (A) WT and WASp^{I294T} PBMCs were freshly isolated from whole blood and monitored for surface L-selectin expression by flow cytometry. Histogram gated on PBMCs reveals comparable levels of L-selectin between patient and control samples. (B) A fixed density of patient or control PBMCs (ie, 3×10^5/mL) were perfused over immobilized sLe^x at 2.5 dyn/cm^2. A single patient sample was analyzed, whereas 3 control samples were analyzed; the average of 3 independent experiments is represented in the histogram. Approximately 30 cells were analyzed per field of view, and an average of 100 cells was analyzed per experiment. Error bar represents SD. (C) Representative example of the jerky nature of PBMC rolling from control and patient samples. Individual cells were tracked for a total of 8 seconds. The superimposed line represents a velocity of 200 μm/s, which is the velocity threshold above which cells are normally considered to be in free flow.

dependent adhesion dynamics as described, we established a cell model for further studies. The 300.19 murine pre–B-cell line has been used extensively to determine the molecular basis of L-selectin–dependent adhesion under flow.[21,25,26] To test the effect of WASp^{I294T} on L-selectin–dependent adhesion, 300.19 cells stably expressing L-selectin were transduced with lentivirus containing open reading frames for EGFP alone, WASp^{WT}-GFP, and WASp^{I294T}-EGFP fusion proteins (which hitherto will be termed WASp^{WT} and WASp^{I294T}). These constructs in which EGFP is N-terminally tagged to WASp have been previously shown not to disrupt WASp activity in vivo.[9]

Flow cytometry confirmed that stable cell lines were close to 100% EGFP$^+$ (Figure 3A). The mean EGFP fluorescence intensity (MFI) of WASp^{I294T} and WASp^{WT} cell lines were comparable, suggesting similar levels of transduction. As previously described,[9] expression of WASp^{WT} or WASp^{I294T} resulted in reduced endogenous WASp expression (Figure 3B), suggesting that the total amount of cellular WASp is tightly controlled at the protein level in cells. As expected, total cellular F-actin was increased in cells expressing WASp^{I294T} compared with WASp^{WT} or EGFP alone (Figure 3C), although WASp^{I294T} protein expression was lower than that of WASp^{WT}: 30% and 70% reduction in sorted low- and high-expressing populations, respectively (Figure 3B). Lower levels of WASp^{I294T} expression in stable cell lines have previously been described and are possibly attributed to reduced stability of the mutant protein.[9] A small but significant increase in F-actin was also seen in cells expressing WASp^{WT} compared with cells expressing EGFP alone. Importantly, surface levels of L-selectin remained constant between the different cell lines (Figure 3D), suggesting that exogenous expression of WASp and/or EGFP did not affect L-selectin turnover from the plasma membrane, which could be influenced by endoproteolytic cleavage.[27]

Expression of WASp^{I294T} alters F-actin remodeling and plasma membrane topography in 300.19 pre-B cells, and is independent of ERM activation

Using SEM, we determined whether 300.19 cells stably expressing WASp^{WT} or WASp^{I249T} possessed altered actin-based membrane structures compared with controls. Indeed, as seen in primary WASp^{I249T} lymphocytes, membrane protrusions in WASp^{I294T}-expressing 300.19 cells were more complex than WASp^{WT}-expressing cells, with significantly more dysmorphic membrane structures and fewer fingerlike "normal" microvilli ($P < .05$ for both; Figure 4A-B). Abnormal microvillus structure on WASp^{I249T} cells frequently appeared as branched, broad, or fused structures (Figure 4A arrowhead). The ERM family of cytoskeleton/membrane-linker proteins are known to be involved in the formation and maintenance of lymphocyte microvilli.[20,28] Interestingly, a previous report had shown interaction between the highly ubiquitously expressed neuronal (N)–WASp and ERM.[29] Based on these previous observations, Western blotting of whole-cell lysates derived from stable cell lines were examined for changes in total ERM levels and C-terminally phosphorylated ERM (which is a hallmark of ERM activation[30]). Immunodetection of the phosphorylated ERM species revealed no difference in ERM activity

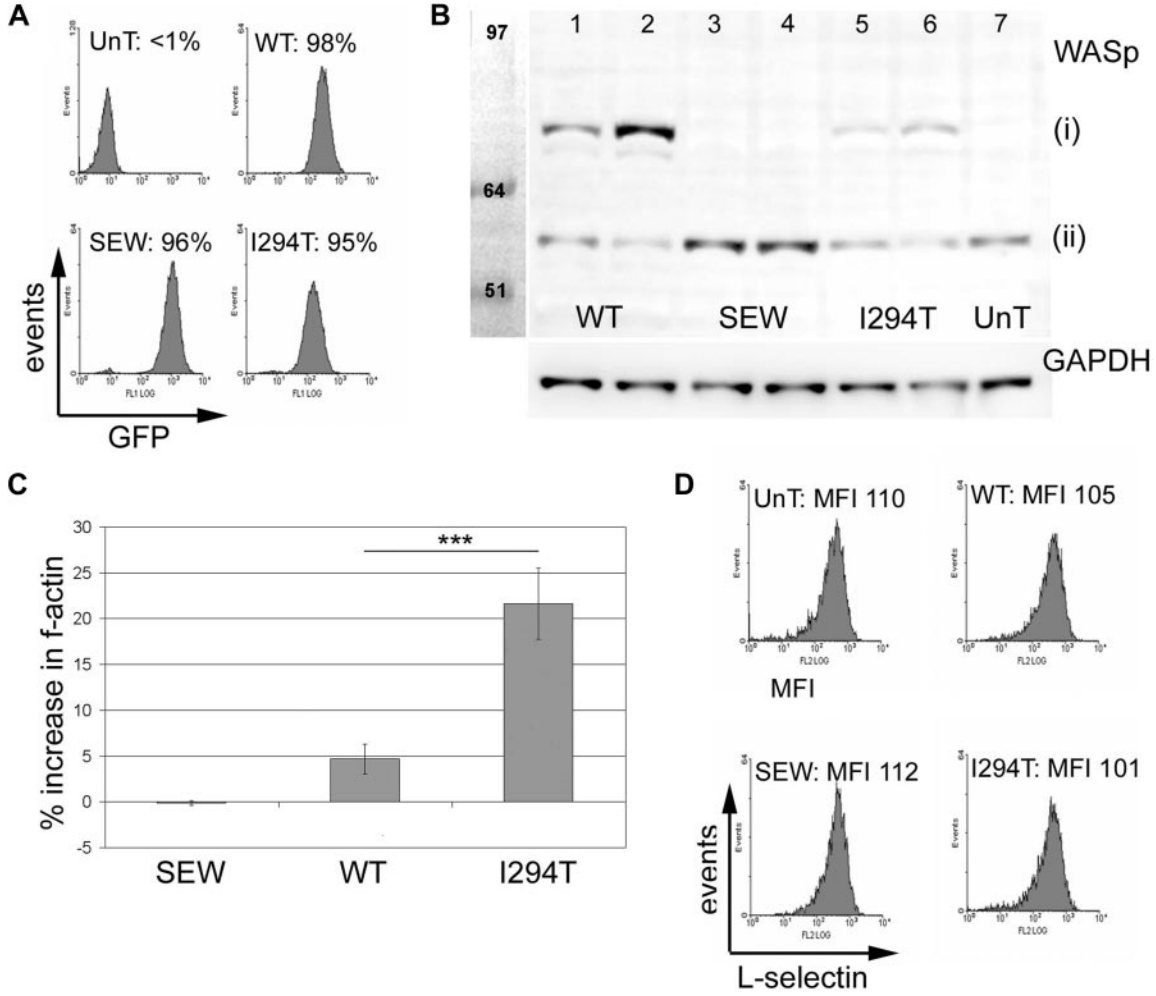

Figure 3. WASp^{I294T} 300.19 cells demonstrate increased levels of F-actin but express normal levels of surface L-selectin. (A) Flow cytometry histograms showing EGFP expression in murine 300.19 pre-B cells before (UnT) and after transfection with lentivirus encoding EGFP alone (SEW), WASp^{WT}, or WASp^{I294T}. WASp^{WT}- and WASp^{I294T}-transfected lines expressing EGFP had average MFI values of 61.8 and 106.7, respectively. Average MFI for EGFP-expressing cells (SEW) was 298.2. (B) Western blot of transfected and untransfected cells showing (i) EGFP-WASp fusion proteins and (ii) endogenous WASp. Lanes 1, 3, and 5 represent cell lines sorted for low EGFP MFI. Lanes 2, 4, and 6 represent cell lines sorted for high EGFP expression. GAPDH levels were monitored for equivalent loading (bottom panel). Relative expression levels were measured using densitometry readings and correction for loading variation. Normalized densitometry readings for EGFP-WASp^{WT} and EGFP-WASp^{I294T} were 147486 and 549950 (lanes 1 and 2) and 101303 and 177848 (lanes 5 and 6), respectively. Immunoblots are representative of 3 independent experiments. (C) F-actin levels were compared between EGFP$^+$ transduced and EGFP$^+$ untransduced cells in the same tube by flow cytometry. WASp^{I294T} cells demonstrate a significant increase in F-actin content compared with cells expressing WASp^{WT} ($P = .001$; 2-tailed t test). There was a small but significant increase in F-actin in WASp^{WT} cells compared with SEW cells ($P = .004$; 2-tailed t test). Error bars represent SD. ***$P = .001$. (D) Untransduced and transduced cells were labeled for L-selectin and analyzed by flow cytometry. Comparable levels of surface L-selectin expression were seen for all cell lines; average MFIs for 3 experiments are shown. All experiments in panels A, C, and D were performed in triplicate on 3 independent occasions.

between cell lines, suggesting that ERMs do not play a dominant role in mediating the altered microvillar architecture seen in WASp^{I294T}-expressing cells (Figure 4C).

WASp^{I294T}, but not WASp^{WT}, impairs L-selectin–dependent adhesion under flow

To determine whether exogenous expression of WASp^{I294T} in 300.19 cells would mimic the phenotype seen in patient cells, transduced 300.19 cells were subjected to rolling assays under similar conditions used for patient cells. Approximately 30 cells expressing WASp^{WT} could be seen interacting with immobilized sLe^x per field of view (Figure 5A), in keeping with what had been observed with primary control cells. In stark contrast, the number of WASp^{I294T} cells rolling was significantly reduced at approximately 10 cells per field of view ($P < .05$; Figure 5A). Furthermore, the average velocity of the rolling fraction of WASp^{I294T} cells was significantly faster than that of WASp^{WT} cells (Figure 5B). As seen with patient cells, closer inspection of rolling behavior between cell lines revealed that the WASp^{I294T} cells had a propensity to roll with a more jerky nature (Figure 5C). These results demonstrate that WASp^{I294T} 300.19 cells exhibit a similar defect of L-selectin–dependent rolling as primary WASp^{I294T} lymphocytes. Taken together, these findings suggest that the I294T mutation alters L-selectin–dependent adhesion—perhaps via defective anchoring of L-selectin to microvilli, or by altering the intrinsic microvillus architecture. Of note, these findings were not due to a global defect of adhesion because integrin-mediated static adhesion to fibronectin was unaffected (supplemental Figure 2).

Ectopic expression of WASp^{WT} and WASp^{I294T} does not affect ectodomain shedding or surface distribution of L-selectin

Ectodomain shedding of L-selectin occurs very rapidly when leukocytes are activated by chemoattractants, such as interleukin-8 or TNF-α, and is thought to affect the rolling velocity and

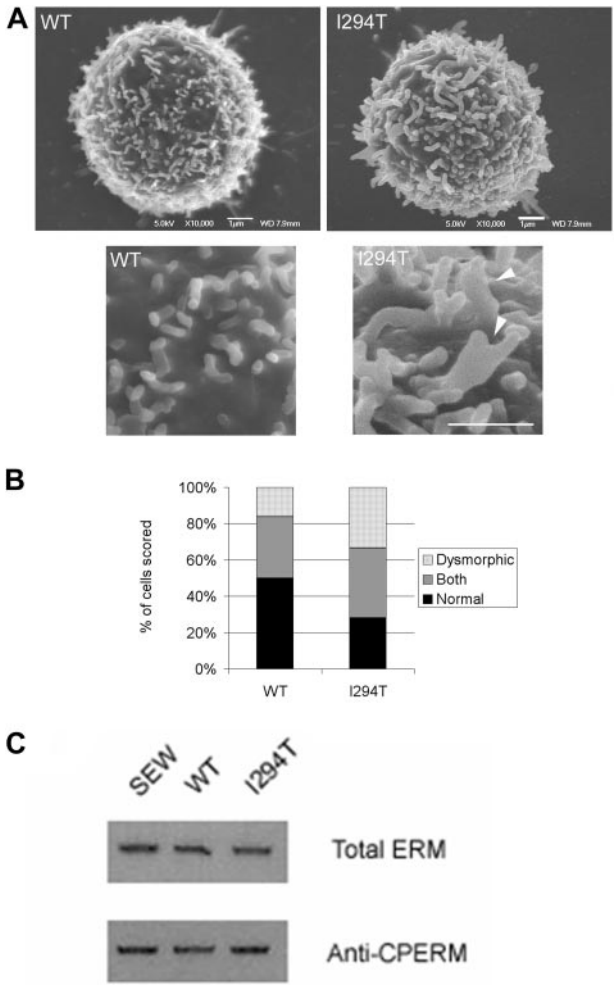

Figure 4. WASp^{I294T} 300.19 cells form dysmorphic microvilli. (A) SEM micrographs of WASp^{WT} and WASp^{I294T} 300.19 cells. Enlarged sections of the same cells are shown in the bottom panels, with dysmorphic microvilli visible in WASp^{I294T} cells (arrowheads). Scale bars represent 1 μm. Images were acquired viewing in a JEOL 6700F FESEM, captured using JEOL software and analyzed with Adobe Photoshop (crop, image size, and brightness/contrast functions only). (B) Cells were blindly scored by 2 independent reseachers for presence of normal fingerlike or dysmorphic broad microvilli. The quantification for at least 50 cells from each condition is shown. WASp^{I294T} cells showed a significantly increased percentage of cells predominantly forming dysmorphic structures and a significantly reduced percentage of cells with a predominance of fingerlike microvilli ($P < .05$ for both; Fisher exact 1-tailed test). (C) Anti–p-ERM Western blotting of extracts derived from 300.19 cells expressing EGFP (SEW), WASp^{WT}, or WASp reveals that overall ERM activity remains unaltered between the cell types. Top panel represents Western blot of p-ERM; bottom panel, total ERM staining to monitor equal loading between samples. Immunoblots are representative of 3 independent experiments.

trafficking potential of neutrophils and T cells, respectively.[23,31,32] To test whether L-selectin shedding could account for the observed rolling defect, cell lines were challenged with increasing amounts of PMA, a potent artificial stimulator of L-selectin shedding. No differences in activation-induced shedding of L-selectin were seen (Figure 6A). Using CD3/CD28 ligation as a more physiologic stimulus, similar levels of L-selectin shedding were also induced in isolated WASp^{I294T} and healthy donor T-lymphocytes (45% vs 51% reduction in MFI; Figure 6B). In addition, incubation of isolated T-lymphocytes with the synthetic sheddase inhibitor Ro-31-9790 augmented L-selectin levels by similar proportions in WASp^{I294T} and healthy donor lymphocytes (48% vs 76% increase in MFI; Figure 6C). It was therefore concluded that WASp is not involved (either positively or negatively) in regulating L-selectin shedding. Attachment of L-selectin to the cortical actin cytoskeleton after activation by antibody cross-linking was also similar between WASp^{I294T} and WASp^{WT} cell lines (supplemental Figure 3), further suggesting that the rolling defects observed related to aberrant microvilli resulting from a primary cytoskeletal defect rather than impairment of L-selectin/cytoskeleton interactions.

The collective observations seen in WASp^{I294T} cells of altered membrane topography and reduced rolling behavior is suggestive of poor (or altered) L-selectin presentation on microvilli. To test this hypothesis, FESEM was used to determine the distribution of L-selectin across the plasma membrane by immunogold labeling. There was no significant difference in the average number of gold particles per micrograph between groups (data not shown), although there was substantial intercell variability within groups (Figure 6E). The percentage of gold particles distributed on cell-surface projections was similar between both groups (78% and 76%, respectively; Figure 6D). As seen with SEM, WASp^{I294T} cells were observed to assemble broad dysmorphic microvilli (Figure 6E asterisk). Enrichment of L-selectin on surface projections and positioning at the tips of microvilli was clearly seen in the majority of WASp^{I294T} and WASp^{WT} cells (Figure 6E arrows), and resembles a classic distribution of L-selectin, which has been previously reported.[21,33] These results imply that ectopic expression of WASp^{WT} or WASp^{I294T} does not lead to altered distribution of L-selectin to microvilli, nor its proteolytic processing from the plasma membrane.

WASp^{I294T} stabilizes L-selectin–dependent adhesion under static conditions

To determine whether L-selectin–ligand interaction is attenuated by WASp^{I294T}, 300.19 cells were plated on to either PLL or sLe^x and subsequently examined by IRM (Figure 7A-B). IRM permits selective visualization of cell-substratum contact points and can be used to measure the turnover of rapidly dynamic adhesion sites.[24] Performing such a technique under flow conditions is technically not possible because the interaction between L-selectin and its ligand would be too transient to capture sufficient adhesive events in real time. The assay was therefore performed under static conditions, allowing continued monitoring of adhesion contact turnover. Cell contacts were imaged using rapid time-lapse microscopy (supplemental Videos 1-4) and assessed for persistence. Stable contacts were defined as those contacts that are present in 3 or 4 of 4 consecutive frames and appear dark gray/black after software analysis (Figure 7), as described in supplemental Methods. In contrast, dynamic (or unstable) contacts are those that appear in only 1 or 2 of 4 consecutive frames and appear light gray after analysis. Cell spreading, as measured by cell circumference, was not different between WASp^{I294T} and WASp^{WT} cells plated on either PLL or sLe^x (data not shown). No difference in the percentage of stable or dynamic adhesions was seen between WASp^{WT} and WASp^{I294T} cells when plated on PLL (Figure 7A,C). In contrast, WASp^{I294T} cells adherent to sLe^x demonstrated a significantly higher percentage of stable adhesions, indicating reduced contact dynamics (Figure 7B-C; $P < .001$). Correspondingly, the percentage of highly dynamic adhesions was significantly lower in WASp^{I294T} cells adherent to sLe^x ($P < .001$), but not PLL (data not shown). In keeping with a slower rate of contact turnover, the total area of contact between cell and substratum (defined as the number of all levels of gray/black pixels visible per cell) was significantly greater for WASp^{I294T} cells than WASp^{WT} cells when plated on sLe^x ($P < .05$), but not on PLL (supplemental Figure 4). Together, these results demonstrate that WASp^{I294T} expression disrupts the dynamics of L-selectin–dependent adhesion turnover

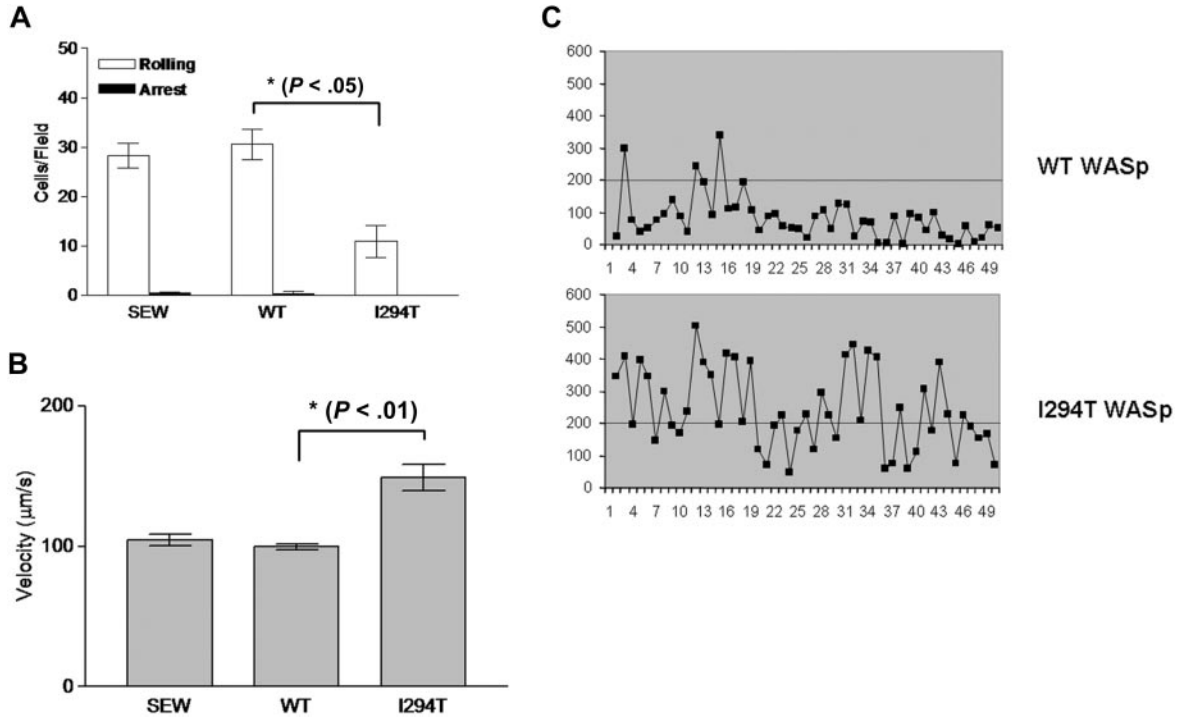

Figure 5. Defective L-selectin–dependent adhesion of WASp^{I294T} cells under flow conditions. 300.19 pre-B cells expressing either EGFP (SEW), WASp^{WT}, or WASp^{I294T} were perfused over immobilized sLe^x in flow chambers. Conditions were optimized for cell rolling (2.5 dyne/cm^2). (A) Dramatic reduction in the number of cells rolling per field of view in cells expressing WASp^{I294T} compared with WASp^{WT} or EGFP-expressing cells (SEW). (B) Average rolling velocity was significantly increased in cells expressing WASp^{I294T}. All error bars represent SD. (C) Compared with WASp^{WT} cells, WASp^{I294} cells demonstrated a jerky rolling behavior characterized by an increase in velocity fluctuation over time. These profiles are comparable with the data presented in Figure 2C. Rolling assays in panels A and B were compiled from 3 independent experiments. The superimposed line represents a velocity of 200 μm/second, which is the velocity threshold above which cells are normally considered to be in free flow.

under static conditions, and raises the possibility that this could manifest in decreased adhesion under flow conditions.

Discussion

The control of WASp activity, like that of its ubiquitous homolog N-WASp, through conformational change is an important mechanism to regulate and spatially direct new F-actin assembly in vivo.[34-36] In this study, we have examined the effect of a previously reported WASp GBD domain mutation (WASp^{I294T}) on lymphocyte function. WASp^{I294T} is predicted to disrupt autoinhibition and has been demonstrated to cause enhanced actin polymerizing activity in vitro, excessive F-actin networks in vivo, and an increase in specific actin-rich structures, such as podosomes, in myeloid cells.[6,7,9]

Here, we have shown that lymphocytes derived from patients expressing WASp^{I294T} and a lymphocyte cell line expressing WASp^{I294T} possess altered microvillous architecture. The role of WASp in lymphocyte microvillous formation is controversial because although impaired microvillous assembly has been repeatedly reported for WASp-null lymphocytes in the context of activation stimuli, it is not clear whether resting WASp-null cells present normal or reduced microvilli.[11-15] These discrepancies may be due to a selective requirement for WASp in response to specific stimuli, or redundancy between WASp family members, particularly N-WASp.[37] Our results in WASp^{I294T} cells, where WASp^{I294T} exerts a dominant effect, indicate that WASp does play a role in lymphocyte microvillous formation, even in the resting state. The phenotype of WASp^{I294T} lymphocytes, which includes both an increase in microvillous density and formation of dysmorphic microvillar structures, most likely results from increased Arp2/3-mediated F-actin formation, although it remains possible that WASp^{I294T} additionally prevents normal localization of endogenous WASp through disrupted interaction with chaperoning binding partners, particularly WASp interacting protein (WIP).

In both primary cells and cell lines, abnormal microvilli were associated with a specific defect of rolling on immobilized sLe^x. Specifically, WASp^{I294T} cells demonstrated a jerky pattern of rolling characterized by marked fluctuations in rolling velocity associated with an increase in average rolling velocity. This phenotype suggests that WASp^{I294T} cells fail to interact efficiently with L-selectin ligand to establish stable rolling. Because L-selectin was expressed at similar levels on microvilli, recruited to the cytoskeleton in similar proportions after activation, and shed with comparable dynamics, in WASp^{WT} and WASp^{I294T} cells, we conclude that these functional defects do not directly result from altered regulation of L-selectin expression. Rather we propose that they are caused by reduced efficiency of contact between dysmorphic microvilli and the ligand-bearing surface. There are 2 main mechanisms by which this might occur. First, L-selectin positioning may be altered on dysmorphic microvilli. Although we found that L-selectin is enriched on microvilli in WASp^{I294T} cells, suggesting normal anchoring to the cytoskeleton, an increase in surface area of densely packed and dysmorphic microvilli may lead to L-selectin dilution at specific membrane regions. Expression of WASp^{I294T} could affect the efficiency and kinetics of L-selectin avidity modulation that is required to support optimal rolling.[38] Second, the collapse and reformation of microvilli during rolling may be retarded by WASp^{I294T}, possibly because of dysregulated F-actin dynamics or as a result of increased microvillous rigidity caused by excessive localized production of cortical F-actin. This is supported by the finding that WASp^{I294T} specifically reduces

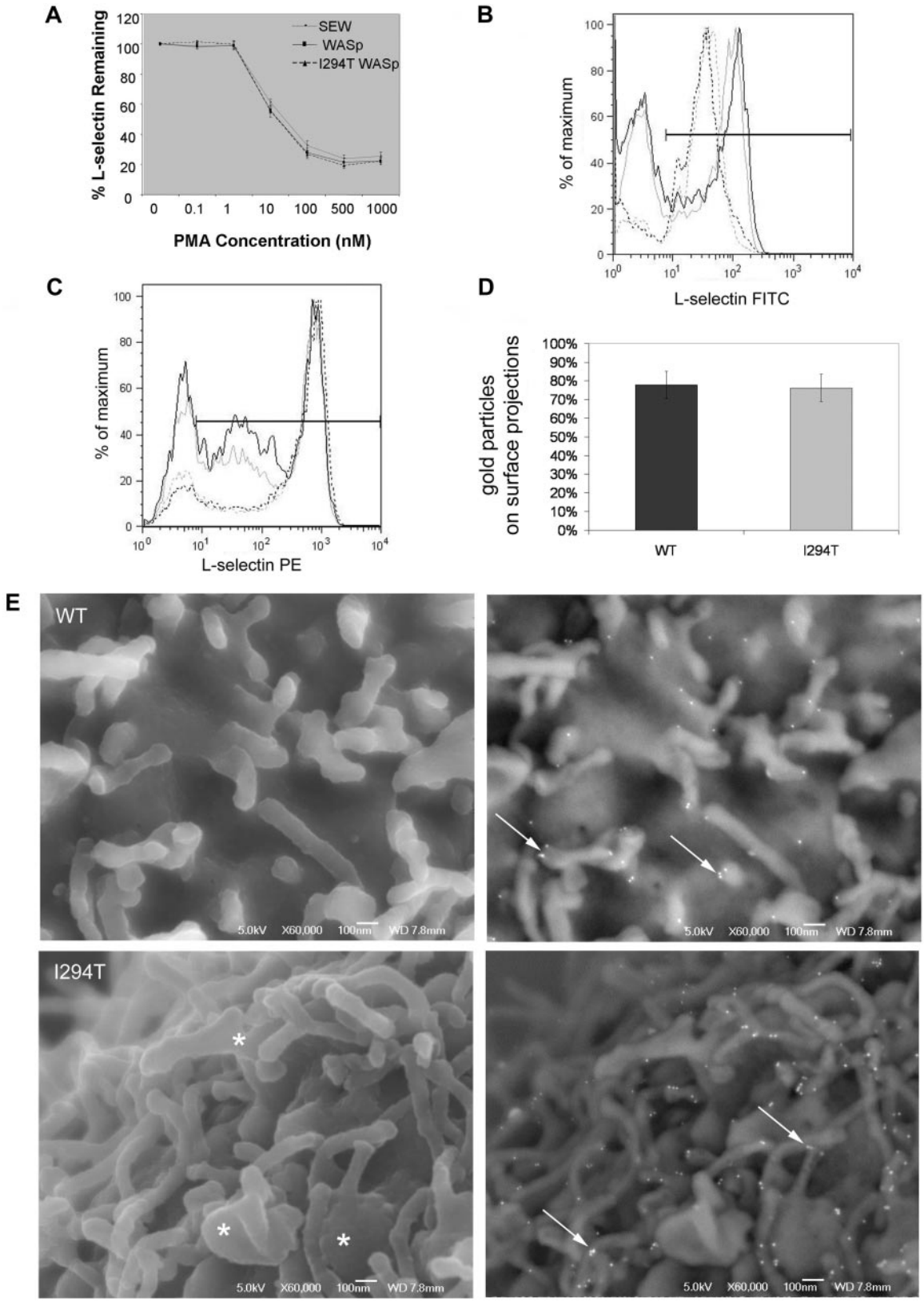

Figure 6. L-selectin shedding and microvillar localization is normal in WASp^{I294T} 300.19 cells. (A) Surface levels of L-selectin were measured by flow cytometry after incubation of cell lines with increasing concentrations of PMA. Normal shedding was induced in all cell lines tested. (B) Surface levels of L-selectin on purified T cells were measured. Representative plots from 1 of 3 experiments are shown. Black lines represent WASp^{I294T} patient cells; gray lines, healthy control cells before (solid lines) and after (dashed lines) incubation with anti-CD3/CD28 beads. The y-axis label "% of maximum" is a normalized measure of the cell count to facilitate overlay comparisons. (C) Surface levels of L-selectin were measured on T cells before (solid lines) and after (dashed lines) incubation with 30μM sheddase inhibitor (Ro-31-9790). Black lines represent WASp^{I294T} patient cells; gray lines, healthy control cells. All error bars represent SD. (D) Surface L-selectin was labeled using immunogold and imaged by FESEM using a JEOL 6700F FESEM and JEOL software. Adobe Photoshop was used for image analysis (crop, image size, and brightness/contrast functions only). Each cell was scored to determine the positioning of individual gold particles on cell body or surface projections. Histogram demonstrates equal distribution of L-selectin on microvilli. (E) FESEM micrographs of WASp^{WT} and WASp^{I294T} 300.19 cells demonstrating surface topography and L-selectin distribution. Secondary electron images detailing morphology are shown in left panels. Dysmorphic, broad microvilli are visible in WASp^{I294T} cells (asterisks). Right panels show backscatter images to detail gold labeling. L-selectin is clearly located and clustered at the tips of microvilli in both WASp^{WT} and WASp^{I294T} cells (arrows). Scale bars represent 100 nm.

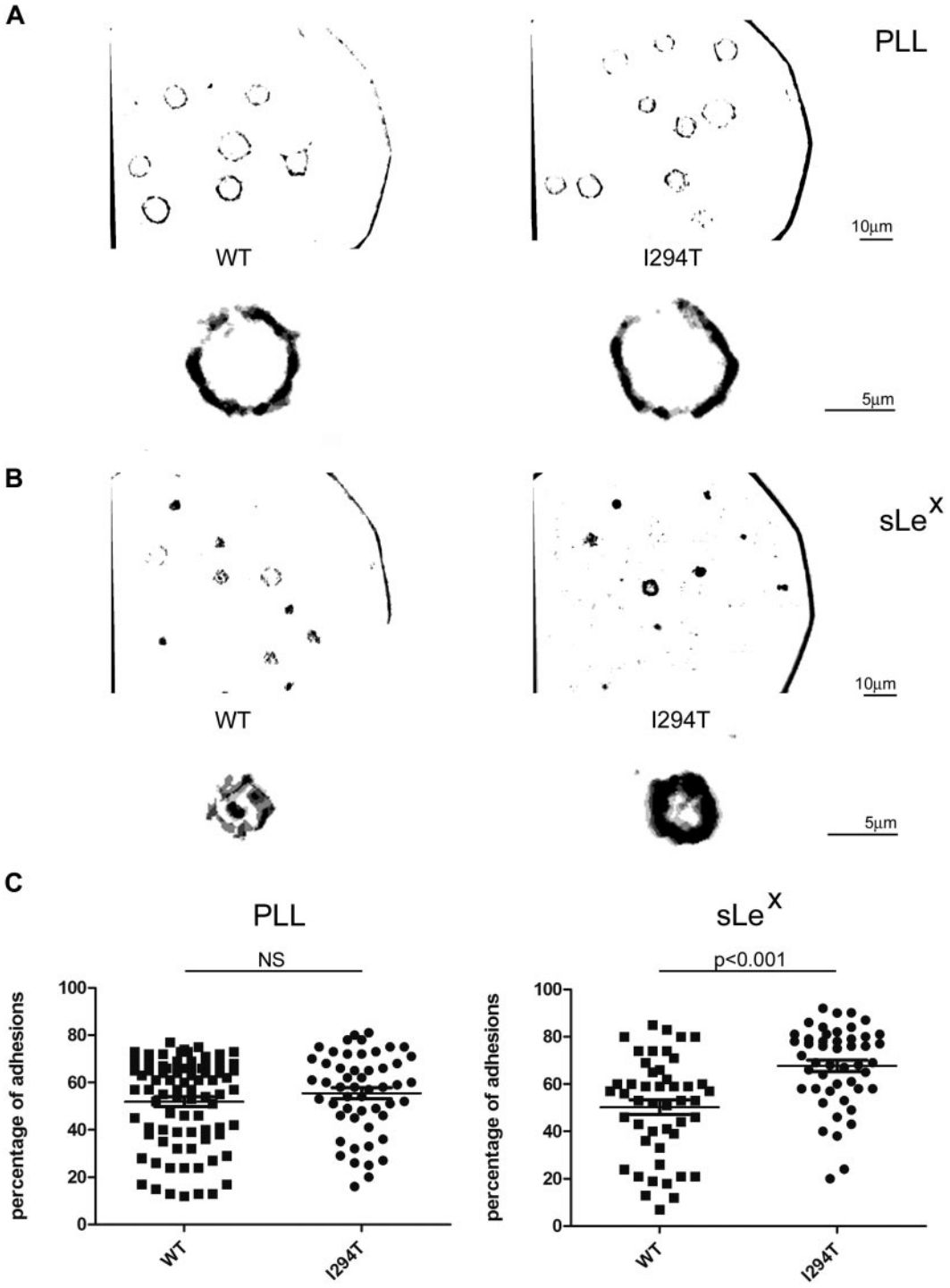

Figure 7. WASp^{I294T} 300.19 cells display altered contact dynamics to L-selectin ligand. (A) WASp^{WT} and WASp^{I294T} 300.19 cells were plated on either PLL or sLe^x (B) and were imaged by rapid time-lapse IRM. sLe^x was immobilized as described in supplemental Methods using glass coverslips. Images were acquired in normal growth medium at 37°C using a Zeiss Standard18 microscope with IV-FL incident light fluorescence attachment, appropriate filters for IRM acquisition, and a Zeiss 63×/1.25 NA Neofluar Antiflex oil-immersion objective and a Pulnix CCD camera (Jai Ltd) using in-house acquisition software (Matrox Video and Imaging Technology Europe Ltd). Composite images of 4 consecutive frames analyzed for adhesion contacts (using Adobe Photoshop as described in supplemental Methods) are shown with a full-field view above an enlarged individual cell. Separate scale bars are shown for original magnification and enlarged images. Stable adhesions appear as black/dark gray pixels, whereas dynamic adhesions appear light gray. WASp^{I294T} cells show an increase in stable adhesions compared with WASp^{WT} cells when adherent to L-selectin ligand (sLe^x) but not to PLL. (C) Stable adhesions were calculated for individual cells and displayed as a percentage of total adhesion pixels. Quantifications of stable adhesions are shown for PLL and sLe^x in left and right panels, respectively. WASp^{I294T} cells demonstrate a significant increase in stable adhesions when adherent to sLe^x but not PLL ($P < .001$; 2-tailed t test).

contact turnover to L-selectin ligand under static conditions. Our IRM findings strongly suggest that dynamic microvillous assembly is abnormal in WASp^{I294T} cells. These findings are consistent with the rolling defects observed in flow assays because microvillous assembly and collapse is required for cell rolling, and it is known that the regulation of rolling velocity in neutrophils relies not only on receptor-ligand interaction but also on cytoskeletal factors.[39] The importance for dynamic cytoskeletal rearrangement in L-selectin–dependent rolling is additionally highlighted by the finding that Rac2-deficient neutrophils are also unable, specifically, to

adhere to L-selectin ligand under flow despite normal levels of L-selectin expression.[40] Indeed, failure to rearrange the cytoskeleton or to disassemble cell-to-substrate contacts under flow gives rise to jerky rolling very similar to that observed in WASp^{I294T} cells here.[39] Furthermore, there is precedence for physical obstruction to cell function caused by increased F-actin concentration, as similar retarding effects were observed for mitosis associated with ectopic nuclear actin filaments in myeloid cells expressing WASp^{I294T} or treated with the F-actin stabilizing drug jasplakinolide.[9]

A total of 11 patients bearing the WASp^{I294T} mutation have been reported worldwide, in 2 studies,[7,8] with a variable clinical phenotype. Disturbance of hematopoiesis are uniform, predominantly affecting neutrophils but also resulting in myelodysplasia and possibly contributing to lymphopenia seen in some patients. Defective hematopoiesis has been attributed, at least in part, to disruption of mitosis by excessive F-actin, resulting in failed cytokinesis.[9] It is also known, however, that adhesion molecules, including L-selectin, mediate cell-cell and cell-matrix adhesions in the bone marrow, which are critical for normal hematopoeisis.[41] Adhesion contacts not only facilitate homing, retention, and release of precursor and mature hematocytes, but are also required for growth signals governing differentiation and survival. L-selectin is expressed on CD34$^+$ stem cells,[42] and although it is not clear what the exact role for L-selectin is during bone marrow development,[41] impaired L-selectin signaling in CD34$^+$ cells is implicated in myelodysplastic syndromes.[43] Our data raise the possibility that WASp^{I294T} may in part perturb hematopoiesis through disruption of normal cell-cell and cell-matrix contacts in bone marrow niches; this warrants further investigation.

At the level of immune cell function in WASp^{I294T}, relatively little is previously known except that podosome assembly is disturbed in myeloid cells, presumably affecting migration.[7] WASp is well described as important for migration in several cell types, and homing defects may be a common factor in immunopathology in WAS.[5] It is plausible from the data presented here that constitutive WASp activation impairs B- and T-cell trafficking in vivo, with implications for induction and maintenance of normal immunity. Although an increased rate of infection in patients bearing the WASp^{I294T} mutation has largely been attributed to neutropenia, infection susceptibility does not correlate closely with the degree of neutropenia, and the most frequent infections reported are of the upper respiratory tract and not those typical of neutrophil dysfunction.[8] Thus, it is certainly possible that other immunodeficiencies contribute, and development of a mouse model for WASP^{I294T} will permit these issues to be addressed. For now, we can conclude that constitutive activation of WASp does affect lymphocyte microvillus formation along with L-selectin–dependent rolling, making it likely that XLN has a clinical phenotype that is not restricted to neutrophils.

Acknowledgments

We would like to thank Kerry Venner (Institute of Neurology, UCL), Peter Munro (Institute of Opthalmology, UCL), and Ayad Eddaoudi and Prabhjoat Chana (Institute of Child Health, UCL) for assistance with SEM, flow cytometry, and cell sorting. We are grateful to Christine Kinnon and Gerben Bouma for critical reading of the manuscript.

A.I., D.M., and A.J.T. are supported by the Wellcome Trust (076834/z/05/z and 057965/Z/99/B). S.O.B. is supported by a grant from the Primary Immunodeficiency Association through the Academy of Medical Sciences. This work was also supported by the Institute of Child Health Biomedical Research Center (S.O.B.) and by Fundacao para a Ciencia e Tecnologia and INOV Contacto, Portugal (J.M. and J.N.).

Authorship

Contribution: S.O.B. and A.I. designed and performed the research and wrote the paper; A.J.T. designed the research and contributed to writing the manuscript; D.J.K., D.A.M., J.M., J.N., and R.R.T. performed research; and A.F. provided essential FESEM expertise.

Conflict-of-interest disclosure: The authors declare no competing financial interests.

Correspondence: Aleksandar Ivetic, Cytoskeleton/Membrane Signalling Group, Cardiovascular Division, King's College London, James Black Centre, 125 Coldharbour La, London SE5 9NU, United Kingdom; e-mail: aleksandar.ivetic@kcl.ac.uk.

References

1. Thrasher AJWA Sp in immune-system organization and function. *Nat Rev Immunol.* 2002;2(9):635-646.
2. Dupre L, Aiuti A, Trifari S, et al. Wiskott-Aldrich syndrome protein regulates lipid raft dynamics during immunological synapse formation. *Immunity.* 2002;17(2):157-166.
3. Lorenzi R, Brickell PM, Katz DR, Kinnon C, Thrasher AJ. Wiskott-Aldrich syndrome protein is necessary for efficient IgG-mediated phagocytosis. *Blood.* 2000;95(9):2943-2946.
4. Burns S, Thrasher AJ, Blundell MP, Machesky L, Jones GE. Configuration of human dendritic cell cytoskeleton by Rho GTPases, the WAS protein, and differentiation. *Blood.* 2001;98(4):1142-1149.
5. Burns S, Cory GO, Vainchenker W, Thrasher AJ. Mechanisms of WASp-mediated hematologic and immunologic disease. *Blood.* 2004;104(12):3454-3462.
6. Devriendt K, Kim AS, Mathijs G, et al. Constitutively activating mutation in WASP causes X-linked severe congenital neutropenia. *Nat Genet.* 2001;27(3):313-317.
7. Ancliff PJ, Blundell MP, Cory GO, et al. Two novel activating mutations in the Wiskott-Aldrich syndrome protein result in congenital neutropenia. *Blood.* 2006;108(7):2182-2189.
8. Beel K, Cotter MM, Blatny J, et al. A large kindred with X-linked neutropenia with an I294T mutation of the Wiskott-Aldrich syndrome gene. *Br J Haematol.* 2009;144(1):120-126.
9. Moulding DA, Blundell MP, Spiller DG, et al. Unregulated actin polymerization by WASp causes defects of mitosis and cytokinesis in X-linked neutropenia. *J Exp Med.* 2007;204(9):2213-2224.
10. Greicius G, Westerberg L, Davey EJ, et al. Microvilli structures on B lymphocytes: inducible functional domains? *Int Immunol.* 2004;16(2):353-364.
11. Kenney D, Cairns L, Remold-O'Donnell E, Peterson J, Rosen FS, Parkman R. Morphological abnormalities in the lymphocytes of patients with the Wiskott-Aldrich syndrome. *Blood.* 1986;68(6):1329-1332.
12. Facchetti F, Blanzuoli L, Vermi W, et al. Defective actin polymerization in EBV-transformed B-cell lines from patients with the Wiskott-Aldrich syndrome. *J Pathol.* 1998;185(1):99-107.
13. Molina IJ, Kenney DM, Rosen FS, Remold-O'Donnell E. T cell lines characterize events in the pathogenesis of the Wiskott-Aldrich syndrome. *J Exp Med.* 1992;176(3):867-874.
14. Gallego MD, Santamaria M, Pena J, Molina IJ. Defective actin reorganization and polymerization of Wiskott-Aldrich T cells in response to CD3-mediated stimulation. *Blood.* 1997;90(8):3089-3097.
15. Westerberg L, Larsson M, Hardy SJ, Fernandez C, Thrasher AJ, Severinson E. Wiskott-Aldrich syndrome protein deficiency leads to reduced B-cell adhesion, migration, and homing, and a delayed humoral immune response. *Blood.* 2005;105(3):1144-1152.
16. Majstoravich S, Zhang J, Nicholson-Dykstra S, et al. Lymphocyte microvilli are dynamic, actin-dependent structures that do not require Wiskott-Aldrich syndrome protein (WASp) for their morphology. *Blood.* 2004;104(5):1396-1403.
17. Hao JJ, Wang G, Pisitkun T, et al. Enrichment of distinct microfilament-associated and GTP-binding-proteins in membrane/microvilli fractions from lymphoid cells. *J Proteome Res.* 2008;7(7):2911-2927.
18. Ley K, Laudanna C, Cybulsky MI, Nourshargh S. Getting to the site of inflammation: the leukocyte adhesion cascade updated. *Nat Rev Immunol.* 2007;7(9):678-689.

19. Erlandsen SL, Hasslen SR, Nelson RD. Detection and spatial distribution of the beta 2 integrin (Mac-1) and L-selectin (LECAM-1) adherence receptors on human neutrophils by high-resolution field emission SEM. *J Histochem Cytochem.* 1993;41(3):327-333.
20. Brown MJ, Nijhara R, Hallam JA, et al. Chemokine stimulation of human peripheral blood T lymphocytes induces rapid dephosphorylation of ERMs which facilitates loss of microvilli and polarization. *Blood.* 2003;102(12):3890-3899.
21. Ivetic A, Florey O, Deka J, Haskard DO, Ager A, Ridley AJ. Mutagenesis of the ezrin-radixin-moesin binding domain of L-selectin tail affects shedding, microvillar positioning, and leukocyte tethering. *J Biol Chem.* 2004;279(32):33263-33272.
22. Demaison C, Parsley K, Brouns G, et al. High-level transduction and gene expression in hematopoietic repopulating cells using a human immunodeficiency [correction of imunodeficiency] virus type 1-based lentiviral vector containing an internal spleen focus forming virus promoter. *Hum Gene Ther.* 2002;13(7):803-813.
23. Lee D, Schultz JB, Knauf PA, King MR. Mechanical shedding of L-selectin from the neutrophil surface during rolling on sialyl Lewis x under flow. *J Biol Chem.* 2007;282(7):4812-4820.
24. Holt MR, Calle Y, Sutton DH, Critchley DR, Jones GE, Dunn GA. Quantifying cell-matrix adhesion dynamics in living cells using interference reflection microscopy. *J Microsc.* 2008;232(1):73-81.
25. Ley K, Tedder TF, Kansas GS. L-selectin can mediate leukocyte rolling in untreated mesenteric venules in vivo independent of E- or P-selectin. *Blood.* 1993;82(5):1632-1638.
26. Dwir O, Kansas GS, Alon R. Cytoplasmic anchorage of L-selectin controls leukocyte capture and rolling by increasing the mechanical stability of the selectin tether. *J Cell Biol.* 2001;155(1):145-156.
27. Smalley DM, Ley K. L-selectin: mechanisms and physiological significance of ectodomain cleavage. *J Cell Mol Med.* 2005;9(2):255-266.
28. Takeuchi K, Sato N, Kasahara H, et al. Perturbation of cell adhesion and microvilli formation by antisense oligonucleotides to ERM family members. *J Cell Biol.* 1994;125(6):1371-1384.
29. Manchanda N, Lyubimova A, Ho HY, et al. The NF2 tumor suppressor Merlin and the ERM proteins interact with N-WASP and regulate its actin polymerization function. *J Biol Chem.* 2005;280(13):12517-12522.
30. Nakamura F, Amieva MR, Furthmayr H. Phosphorylation of threonine 558 in the carboxyl-terminal actin-binding domain of moesin by thrombin activation of human platelets. *J Biol Chem.* 1995;270(52):31377-31385.
31. Hafezi-Moghadam A, Ley K. Relevance of L-selectin shedding for leukocyte rolling in vivo. *J Exp Med.* 1999;189(6):939-948.
32. Galkina E, Tanousis K, Preece G, et al. L-selectin shedding does not regulate constitutive T cell trafficking but controls the migration pathways of antigen-activated T lymphocytes. *J Exp Med.* 2003;198(9):1323-1335.
33. Pavalko FM, Walker DM, Graham L, Goheen M, Doerschuk CM, Kansas GS. The cytoplasmic domain of L-selectin interacts with cytoskeletal proteins via alpha-actinin: receptor positioning in microvilli does not require interaction with alpha-actinin. *J Cell Biol.* 1995;129(4):1155-1164.
34. Miki H, Sasaki T, Takai Y, Takenawa T. Induction of filopodium formation by a WASP-related actin-depolymerizing protein N-WASP. *Nature.* 1998;391(6662):93-96.
35. Lorenz M, Yamaguchi H, Wang Y, Singer RH, Condeelis J. Imaging sites of N-wasp activity in lamellipodia and invadopodia of carcinoma cells. *Curr Biol.* 2004;14(8):697-703.
36. Lim RP, Misra A, Wu Z, Thanabalu T. Analysis of conformational changes in WASP using a split YFP. *Biochem Biophys Res Commun.* 2007;362(4):1085-1089.
37. Westerberg L, Greicius G, Snapper SB, Aspenstrom P, Severinson E. Cdc42, Rac1, and the Wiskott-Aldrich syndrome protein are involved in the cytoskeletal regulation of B lymphocytes. *Blood.* 2001;98(4):1086-1094.
38. Dwir O, Solomon A, Mangan S, Kansas GS, Schwarz US, Alon R. Avidity enhancement of L-selectin bonds by flow: shear-promoted rotation of leukocytes turn labile bonds into functional tethers. *J Cell Biol.* 2003;163(3):649-659.
39. Yago T, Leppanen A, Qiu H, et al. Distinct molecular and cellular contributions to stabilizing selectin-mediated rolling under flow. *J Cell Biol.* 2002;158(4):787-799.
40. Roberts AW, Kim C, Zhen L, et al. Deficiency of the hematopoietic cell-specific Rho family GTPase Rac2 is characterized by abnormalities in neutrophil function and host defense. *Immunity.* 1999;10(2):183-196.
41. Prosper F, Verfaillie CM. Regulation of hematopoiesis through adhesion receptors. *J Leukoc Biol.* 2001;69(3):307-316.
42. Eckfeldt CE, Mendenhall EM, Verfaillie CM. The molecular repertoire of the 'almighty' stem cell. *Nat Rev Mol Cell Biol.* 2005;6(9):726-737.
43. Buccisano F, Maurillo L, Tamburini A, et al. Evaluation of the prognostic relevance of L-selectin and ICAM1 expression in myelodysplastic syndromes. *Eur J Haematol.* 2008;80(2):107-114.